Editors' Suggestion | Featured in Physics

Discovery of Gamma Rays from the Quiescent Sun with HAWC

A. Albert,[1] R. Alfaro,[2] C. Alvarez,[3] J. C. Arteaga-Velázquez,[4] D. Avila Rojas,[2] H. A. Ayala Solares,[5] R. Babu,[6] E. Belmont-Moreno,[2] C. Brisbois,[7] K. S. Caballero-Mora,[3] T. Capistrán,[8] A. Carramiñana,[9] S. Casanova,[10] O. Chaparro-Amaro,[11] U. Cotti,[4] J. Cotzomi,[12] S. Coutiño de León,[13] E. De la Fuente,[14] R. Diaz Hernandez,[9] B. L. Dingus,[1,7] M. A. DuVernois,[13] M. Durocher,[1] J. C. Díaz-Vélez,[14] R. W. Ellsworth,[7] K. Engel,[7] C. Espinoza,[2] K. L. Fan,[7] K. Fang,[13] M. Fernández Alonso,[5] H. Fleischhack,[15,16,17] N. Fraija,[8] J. A. García-González,[18] F. Garfias,[8] M. M. González,[8] J. A. Goodman,[7] J. P. Harding,[1] S. Hernandez,[2] J. Hinton,[19] D. Huang,[6] F. Hueyotl-Zahuantitla,[3] P. Hüntemeyer,[6] A. Iriarte,[8] V. Joshi,[20] S. Kaufmann,[21] J. Lee,[22] J. T. Linnemann,[23] A. L. Longinotti,[8] G. Luis-Raya,[21] K. Malone,[24] O. Martinez,[12] J. Martínez-Castro,[11] J. A. Matthews,[25] P. Miranda-Romagnoli,[26] J. A. Morales-Soto,[4] E. Moreno,[12] M. Mostafá,[5] A. Nayerhoda,[10] L. Nellen,[27] M. U. Nisa,[23,*] R. Noriega-Papaqui,[26] L. Olivera-Nieto,[19] N. Omodei,[28] Y. Pérez Araujo,[8] E. G. Pérez-Pérez,[21] C. D. Rho,[29] D. Rosa-González,[9] E. Ruiz-Velasco,[19] H. Salazar,[12] D. Salazar-Gallegos,[23] A. Sandoval,[2] M. Schneider,[7] J. Serna-Franco,[2] A. J. Smith,[7] Y. Son,[22] R. W. Springer,[30] O. Tibolla,[21] K. Tollefson,[23] I. Torres,[9] R. Torres-Escobedo,[31] R. Turner,[6] F. Ureña-Mena,[9] E. Varela,[12] L. Villaseñor,[12] X. Wang,[6] I. J. Watson,[22] E. Willox,[7] S. Yun-Cárcamo,[32] H. Zhou,[31] and C. de León[4]

(HAWC Collaboration)

J. F. Beacom,[33,34,35] T. Linden,[36] K. C. Y. Ng,[37] A. H. G. Peter,[33,34,35,38] and B. Zhou[39]

[1]*Physics Division, Los Alamos National Laboratory, Los Alamos, New Mexico 87544, USA*
[2]*Instituto de Física, Universidad Nacional Autónoma de México, Ciudad de México, Mexico*
[3]*Universidad Autónoma de Chiapas, Tuxtla Gutiérrez, Chiapas, Mexico*
[4]*Universidad Michoacana de San Nicolás de Hidalgo, Morelia, Mexico*
[5]*Department of Physics, Pennsylvania State University, University Park, Pennsylvania, USA*
[6]*Department of Physics, Michigan Technological University, Houghton, Michigan, USA*
[7]*Department of Physics, University of Maryland, College Park, Maryland, USA*
[8]*Instituto de Astronomía, Universidad Nacional Autónoma de México, Ciudad de México, Mexico*
[9]*Instituto Nacional de Astrofísica, Óptica y Electrónica, Puebla, Mexico*
[10]*Instytut Fizyki Jadrowej im Henryka Niewodniczanskiego Polskiej Akademii Nauk, IFJ-PAN, Krakow, Poland*
[11]*Centro de Investigación en Computación, Instituto Politécnico Nacional, Mexico City, Mexico*
[12]*Facultad de Ciencias Físico Matemáticas, Benemérita Universidad Autónoma de Puebla, Puebla, Mexico*
[13]*Department of Physics, University of Wisconsin-Madison, Madison, Wisconsin, USA*
[14]*Departamento de Física, Centro Universitario de Ciencias Exactase Ingenierias, Universidad de Guadalajara, Guadalajara, Mexico*
[15]*Department of Physics, Catholic University of America, 620 Michigan Avenue NE, Washington, DC 20064, USA*
[16]*NASA Goddard Space Flight Center, Greenbelt, Maryland 20771, USA*
[17]*Center for Research and Exploration in Space Science and Technology, NASA/GSFC, Greenbelt, Maryland 20771*
[18]*Tecnologico de Monterrey, Escuela de Ingeniería y Ciencias, Avenue Eugenio Garza Sada 2501, 64849 Monterrey, N.L., Mexico*
[19]*Max-Planck Institute for Nuclear Physics, 69117 Heidelberg, Germany*
[20]*Erlangen Centre for Astroparticle Physics, Friedrich-Alexander-Universität Erlangen-Nürnberg, Erlangen, Germany*
[21]*Universidad Politecnica de Pachuca, Pachuca, Hgo, Mexico*
[22]*University of Seoul, Seoul, Republic of Korea*
[23]*Department of Physics and Astronomy, Michigan State University, East Lansing, Michigan, USA*
[24]*Space Science and Applications Group, Los Alamos National Laboratory, Los Alamos, New Mexico 87544, USA*
[25]*Department of Physics and Astronomy, University of New Mexico, Albuquerque, New Mexico, USA*
[26]*Universidad Autónoma del Estado de Hidalgo, Pachuca, Mexico*
[27]*Instituto de Ciencias Nucleares, Universidad Nacional Autónoma de México, Ciudad de México, Mexico*
[28]*Department of Physics, Stanford University, Stanford, California 94305–4060, USA*
[29]*Department of Physics, Sungkyunkwan University, Suwon 16419, South Korea*
[30]*Department of Physics and Astronomy, University of Utah, Salt Lake City, Utah, USA*
[31]*Tsung-Dao Lee Institute & School of Physics and Astronomy, Shanghai Jiao Tong University, Shanghai, People's Republic of China*
[32]*Department of Physics, University of Maryland, College Park, Maryland, USA*
[33]*Center for Cosmology and AstroParticle Physics (CCAPP), The Ohio State University, Columbus, Ohio 43210, USA*
[34]*Department of Physics, The Ohio State University, Columbus, Ohio 43210, USA*
[35]*Department of Astronomy, The Ohio State University, Columbus, Ohio 43210, USA*

[36]The Oskar Klein Centre, Department of Physics, Stockholm University, AlbaNova, SE-10691 Stockholm, Sweden
[37]Department of Physics, The Chinese University of Hong Kong, Sha Tin, Hong Kong, China
[38]School of Natural Sciences, Institute for Advanced Study, 1 Einstein Drive, Princeton, New Jersey 08540, USA
[39]William H. Miller III Department of Physics and Astronomy, Johns Hopkins University, Baltimore, Maryland 21218, USA

(Received 6 December 2022; revised 27 January 2023; accepted 23 June 2023; published 3 August 2023)

We report the first detection of a TeV γ-ray flux from the solar disk (6.3σ), based on 6.1 years of data from the High Altitude Water Cherenkov (HAWC) observatory. The 0.5–2.6 TeV spectrum is well fit by a power law, $dN/dE = A(E/1\,\mathrm{TeV})^{-\gamma}$, with $A = (1.6 \pm 0.3) \times 10^{-12}$ TeV^{-1} cm^{-2} s^{-1} and $\gamma = 3.62 \pm 0.14$. The flux shows a strong indication of anticorrelation with solar activity. These results extend the bright, hard GeV emission from the disk observed with Fermi-LAT, seemingly due to hadronic Galactic cosmic rays showering on nuclei in the solar atmosphere. However, current theoretical models are unable to explain the details of how solar magnetic fields shape these interactions. HAWC's TeV detection thus deepens the mysteries of the solar-disk emission.

DOI: 10.1103/PhysRevLett.131.051201

The Sun is one of the most widely studied sources in multimessenger astrophysics. It can be probed in detail through direct observations across the electromagnetic spectrum, in MeV-scale neutrinos, and in accelerated particles, as well as indirectly through helioseismology, its cosmic-ray shadow, and magnetic field measurements [1,2].

However, the Sun's emission at high energies challenges present models. For example, Fermi Large Area Telescope (LAT) observations [3–7] (building on earlier hints from EGRET [8]) show that the solar disk is a bright, continuous source of gamma rays between 0.1 and 200 GeV, revealing several puzzling features. The primary emission mechanism seems to be the decay of π^0 produced by the scattering of hadronic Galactic cosmic rays with nuclei in the solar atmosphere over the full disk, with the requirement that the cosmic rays must first be converted from incoming to outgoing by magnetic fields [9]. Without this magnetic redirection, cosmic rays would only be grazing the surface of the Sun, encountering limited column density, and the disk emission would be much fainter [10]. Even so, compared with theoretical expectations [9–14], the observed flux of gamma rays from the solar disk is brighter, and the spectrum has been found to be harder (with an unexplained dip near 40 GeV) [3,4,6]. Additionally, the flux is anticorrelated with solar activity, and the emission across the disk appears to be nonuniform [5,7].

Decisive new probes are needed to solve these puzzles, and observations at high energies are especially important, for multiple reasons. Unlike the cosmic-ray spectrum, which falls as $\sim E^{-2.7}$, the solar-minimum γ-ray spectrum (except for the dip) falls as $\sim E^{-2.2}$ up to at least 200 GeV. This trend must eventually reach a break energy, where cosmic rays are no longer sufficiently deflected in the Sun's magnetic field, providing an important clue to the details of their propagation. Separately, the highest-energy gamma rays are likely produced at the greatest depths under the photosphere ($\sim$1000 km), thus providing sensitivity to otherwise-hidden magnetic fields [9]. Last, understanding the solar emission will be important for tests of new physics, including dark matter [15–19].

In this Letter, we use observations with the High Altitude Water Cherenkov (HAWC) observatory to probe the solar disk in the TeV range. We substantially improve upon the earlier HAWC search that set an upper limit on the γ-ray flux [20] (ARGO-YBJ also set a limit [21]). We use a larger dataset, better reconstruction algorithms, and new signal-isolation techniques. In the following, we describe the HAWC data, our analysis methods, tests of the time variation and spectrum slope, and then conclude. Further details are given in Supplemental Material [22], which also includes Refs. [23–25].

HAWC data.—The HAWC observatory, located at an altitude of 4100 m near Puebla, Mexico, is designed to detect multi-TeV cosmic rays and gamma rays through atmospheric-shower secondary particles that reach the ground [26–28]. These secondaries are detected in an array of 300 detector units that employ the water-Cherenkov technique and operate nearly continuously. The vast majority of detected showers are induced by hadronic cosmic rays, which cause a near-isotropic and near-constant background. In searches for gamma-ray-induced showers, the cosmic-ray background can be greatly reduced (to a fraction 10^{-1} to 10^{-4}, depending on the energy of the primary particle) and any γ-ray signals nearly perfectly preserved, by cuts based on shower topology (γ-ray showers are compact, while hadronic showers have a broader and clumpier footprint) [27]. The angular resolution of HAWC depends on the energy and zenith angle, ranging from $\sim$1° at 1 TeV to 0.2° above 10 TeV (see the Supplemental Material [22]). HAWC's γ-ray observations, which cover the entire sky at zenith angles 0–45°, offer excellent sensitivity to both source and diffuse emission, as has been exploited in a variety of studies (see, e.g., Refs. [28–34]).

HAWC is among the few detectors capable of observing the Sun in the TeV range [20]. Its large field of view and high livetime fraction allow continuous exposure as the Sun transits across the sky. Compared with the earlier HAWC analysis, here we make significant improvements. First, we use a larger and more varied exposure, spanning November 2014 to January 2021 (6.1 years). The first half of the data corresponds to an active but declining part of solar cycle 24, while the second half corresponds to the minimum of solar cycle 25; this long baseline thus allows for tests of time variability. Second, we use an improved offline reconstruction sample (Pass 5, compared with Pass 4 in previous work [20]) with new calibrations and better algorithms. The new data have superior angular resolution and background rejection, particularly at low energies, improving the sensitivity by a factor of ∼2–5, depending on the source spectrum (see Fig. S1 in the Supplemental Material [22]). Third, we use a new, data-driven approach to separate the γ-ray signal from backgrounds, taking into account the suppression of cosmic-ray fluxes from directions near the Sun (the shadow effect).

Main analysis.—To search for TeV-range γ-ray emission from the solar disk, we develop a simple but powerful analysis technique that measures the signal and background independently.

We select only well-reconstructed events with shower cores within the fiducial area of HAWC [34]. We cut Milky Way sources and diffuse γ-ray emission by excluding times when the Sun is within $\pm 10°$ of the Galactic plane. The exposure is 1872 days, following the cuts. Extragalactic γ-ray emission is minor and is smeared into the background as we track the Sun across the sky. None of the significantly detected blazars in HAWC data intersect the Sun's path [35]. The fluxes of isotropic electron cosmic rays and the directional gamma rays they produce by inverse-Compton scattering of solar photons are both negligible in the TeV range [10,36–38].

We bin the data into 11 analysis bins based on the fraction of the detector array triggered. Higher-energy events trigger a larger fraction of the array, corresponding to higher-numbered bins; however, the energy resolution (≃50–100%) is large enough that the bins are partially correlated. We use Bx to denote analysis bin x. Table 1 in the Supplemental Material [22] gives the details of these bins.

Following the steps detailed below, we estimate the excess of γ-ray events at the moving solar position. We obtain the spatial distribution of the data using the background-estimation and skymap-making procedures of Refs. [20,39]. Prior to any gamma-hadron separation cuts, the data are dominated by hadronic cosmic rays. In general, a γ-ray source appears as an excess of events in a particular direction after gamma-hadron separation cuts. Near the Sun, the analysis is complicated by an anisotropy in the background called the "Sun shadow," where some Galactic cosmic rays, with energies between 1 and 1000 TeV, are blocked by the Sun. The shadow is not perfectly round, and it has a slightly displaced position; these effects are due to deflections of cosmic rays in the Sun's coronal fields and in the interplanetary magnetic field [40,41]. Our new analysis —validated on simulations and on observations of the Moon shadow—takes the Sun shadow into account, overcoming a limiting systematic of our previous work [20].

To isolate any disk signal we must accurately subtract the expected shadow, which takes three steps, as we illustrate for the example of $B3$. At each step, for every pixel i in the map, we record the number of data events N_i, the number of background events $\langle N_i \rangle$, and report the fractional deviation relative to the background, calculating the significance following Ref. [42]. The fractional deviation is given by $N_i/\langle N \rangle_i - 1$ and shows the amplitude of the deficit (or excess) in the pixel i.

(1) Figure 1 (top row) shows the map for the cosmic-ray dominated data (before gamma-hadron cuts). This step measures the shadow's spatial profile and amplitude with high statistics. Before the gamma-hadron cuts, there are 4.0×10^4 fewer events within a 1.1° region of interest around the Sun (comparable to the 1-σ width of the shadow) than the 5.5×10^6 expected from the isotropic background. Figure 1 (top row) also shows the angular profile centered on the Sun.

(2) Figure 1 (middle row) shows the same results after gamma-hadron cuts. If there were no shadow, this step would yield our results for the disk emission. However, the shadow persists because the data are still cosmic-ray dominated, though the shadow significance is less and there may be a positive contribution from disk emission. There are now 6.7×10^3 fewer events within the region of interest than the 1.7×10^6 expected from background. The true shadow profile measured in step one needs to be subtracted from these data to reveal any positive contribution from gamma rays.

(3) Figure 1 (bottom row) shows what remains after we subtract (in two dimensions) the rescaled shadow map measured in the top row from the gamma-hadron cut data in the middle row. The rescaling takes into account the reduced number of events following the cuts. There is now an excess of 6.3×10^3 events in the region of interest relative to the background. In the absence of a γ-ray signal, this step should result in a residual consistent with the isotropic background and statistical fluctuations. In the presence of a γ-ray signal centered on the Sun, there should be an excess relative to the background, with a smoothly falling radial profile. The event counts in each pixel are subject to Poisson errors and are propagated as such during the shadow subtraction.

We repeat these steps for all analysis bins used in this work. In $B2$ (median energy 0.6 TeV), we detect a γ-ray excess at a significance of 4.2σ. In $B3$ (1 TeV), the excess is 4.5σ, and in $B4$ (1.7 TeV), it is 5.1σ. These significance values, based on the number of excess γ-ray events above

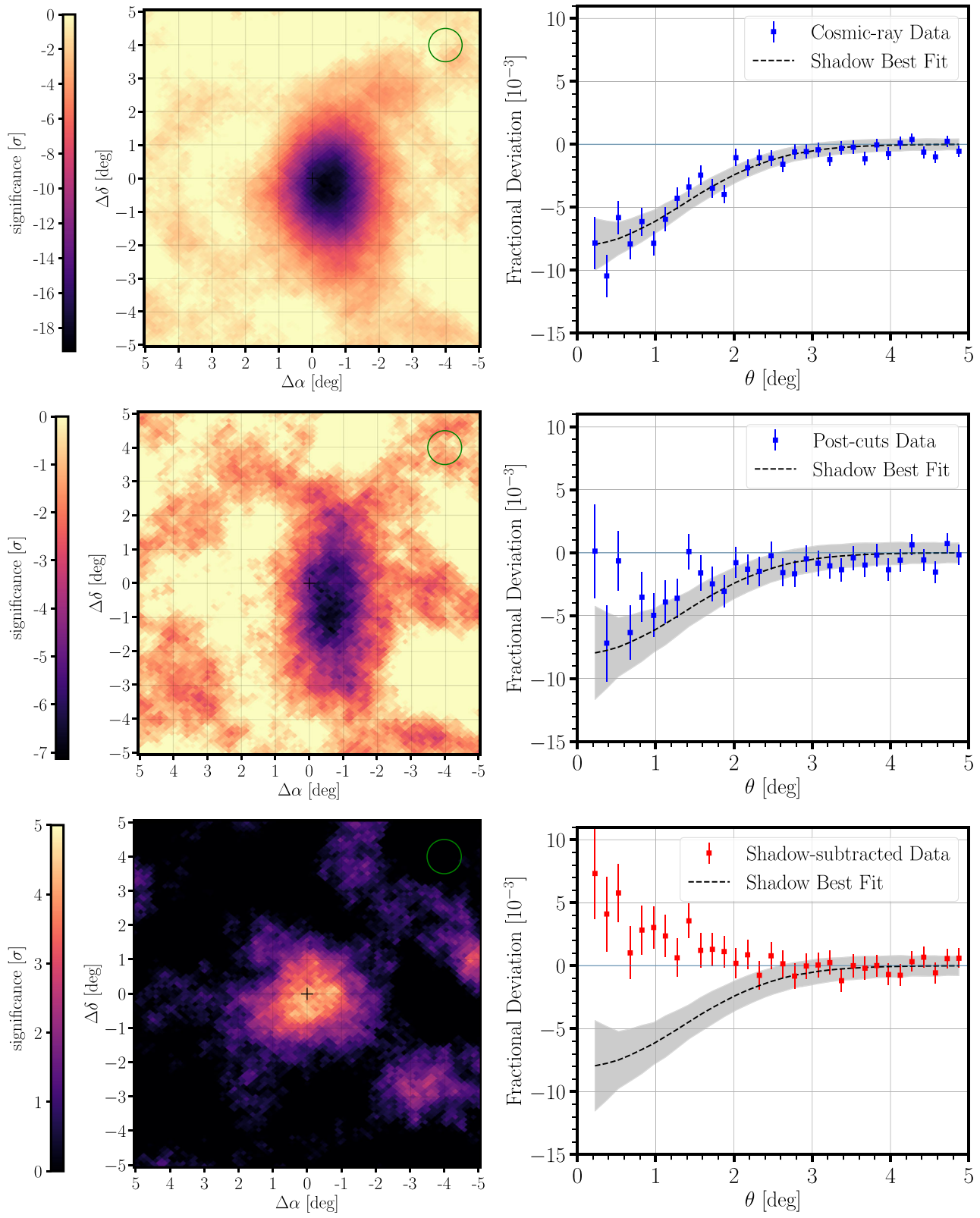

FIG. 1. Results for the example of bin $B3$. Left: significance maps in Sun-centered coordinates for 6.1 years of data, smoothed with a 1° top-hat function for visual clarity. The green circle illustrates the true point spread function. Right: angular profiles (steps of 0.15° from the Sun) of the fractional deviation from background. The black dashed line shows the projection of the best-fit 2D Gaussian model fitted to the shadow, with the shaded band indicating the total uncertainty in the model. The top row shows the cosmic-ray dominated data. The middle row shows the events that survive the gamma-hadron separation cuts. The bottom row is after subtracting the measured cosmic-ray shadow (see top-row data) from the middle-row data, leaving a γ-ray excess at the position of the Sun (marked by a cross).

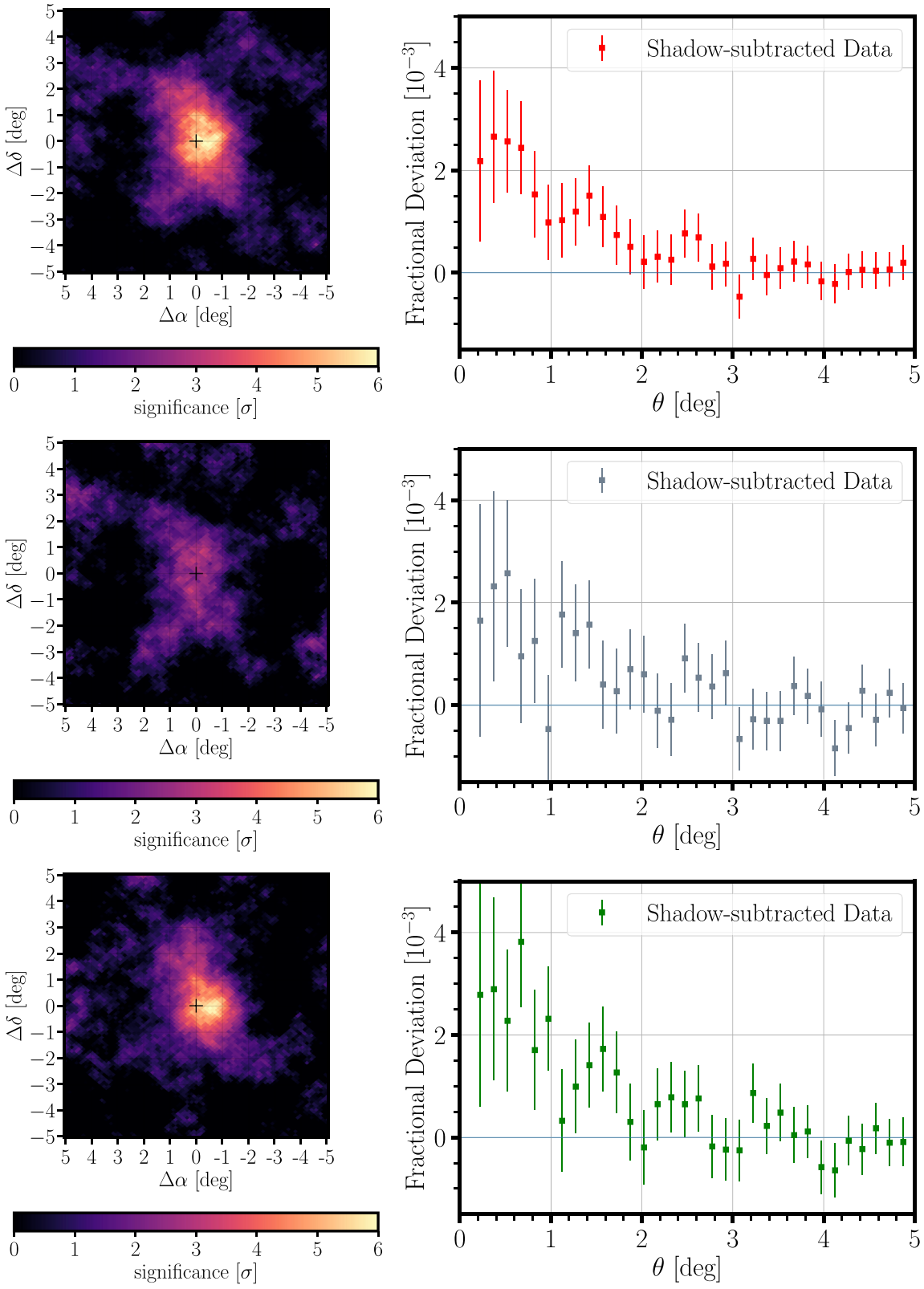

FIG. 2. Results for the combination of bins $B2$, $B3$, and $B4$. Top: the full 6.1-year data. Middle: solar-maximum period. Bottom: solar-minimum period.

the isotropic background, are calculated using the Li and Ma method [42]. The combined significance of the excess in these three bins is 6.3σ, exceeding requirements for a discovery. No significant excesses are observed in the lower-energy bins (where the gamma-hadron separation and angular resolution worsen) or the higher-energy bins (where the statistics worsen); further details are given in the Supplemental Material [22].

A key advantage of our new analysis technique is that it allows separate measurements of the background (before gamma-hadron cuts) and a potential signal (after gamma-hadron cuts) for the same exposure in terms of sky directions and durations. Another is that it directly and model independently measures the shadow from data, without needing any time-dependent theoretical modeling of its complex details.

A potential systematic effect in our analysis could be oversubtracting the shadow, which would result in an artificial signal. We perform several cross-checks to test for this possibility, finding no problems. Further details are given in the Supplemental Material [22].

For off-Sun regions, we simulate the effects of a shadow, which we subtract following the procedures above. We find no evidence of spurious γ-ray sources due to oversubtraction.

We repeat this, but now also simulate the effects of a point source of flux 2×10^{-12} TeV^{-1} cm^{-2} s^{-1} at 1 TeV and spectrum falling as E^{-3}, placed within the simulated shadow. We find that we can recover this source with significance $> 6\sigma$.

HAWC observes a significant cosmic-ray shadow for the moon [43]. We repeat the entire analysis using data around the moon with the same exposure as in the main analysis and find no evidence of γ-ray emission.

Time variation.—We test for time dependence in the signal by analyzing the data split into two halves: Nov. 2014 to Dec. 2017 (closer to solar maximum, 914 days) and Jan. 2018 to Jan. 2021 (nearly matching solar minimum, 972 days).

Figure 2 shows the maps and angular profiles for the full 6.1 years of data (left), solar maximum (middle), and solar minimum (right). Here we combine bins $B2$, $B3$, and $B4$. We find a strong indication of time variation. For the solar-maximum data, we find evidence for a weak signal (3.3σ), but for the solar-minimum data, we detect a strong signal (5.9σ). We also find that the flux during the solar minimum is higher than the 6.1-year average (calculated below). Qualitatively, these results match the time variation seen in the Fermi-LAT data [4–6]. The fact that the flux is anticorrelated with solar activity over energies 0.1 GeV to ~1 TeV, without an obvious energy dependence, is an important clue for theoretical modeling.

Spectrum.—We use a forward-folded maximum-likelihood approach to obtain the flux of gamma rays from the shadow-subtracted data. Using the HAWC plug in to the

TABLE I. The best-fit parameters and TS values for each of the three time periods analyzed. The reported uncertainties are statistical.

Data	$A \times 10^{-12}$ (TeV^{-1} cm^{-2} s^{-1})	γ	r (deg.)	TS
6.1 yr	1.6 ± 0.3	3.62 ± 0.14	0.24 ± 0.1	45
Solar maximum	1.3 ± 1.1	3.9 ± 0.4	0.24 (fixed)	8.8
Solar minimum	4.0 ± 0.7	3.52 ± 0.14	0.24 (fixed)	33.1

Multi-Mission Maximum Likelihood framework [44–46], we fit for a source described by a disk of variable radius r and a spectrum given by

$$\frac{dN}{dE} = A\left(\frac{E}{E_0}\right)^{-\gamma}, \tag{1}$$

where A is the differential flux at the reference energy E_0 (1 TeV) and γ is the spectral index.

The log-likelihood function $\mathcal{L}(A, \gamma, r)$ encodes the Poisson probability of observing D_p events in each pixel p, given a source flux model that depends on the parameters A, γ, and r. It is written as

$$\mathcal{L}(A, \gamma, r) = \sum_{b=2}^{8} \sum_{p=1}^{N} \log\left\{\frac{[B_p + S_p(A, \gamma, r)]^{D_p}}{D_p!}\right\} - [B_p + S_p(A, \gamma, r)], \tag{2}$$

where B_p is the expected number of background events in the spatial pixel p and S_p is the number of signal events under the assumed flux model. For the fit, we use all $N = 5940$ pixels within 5° of the Sun. To obtain the best-fit

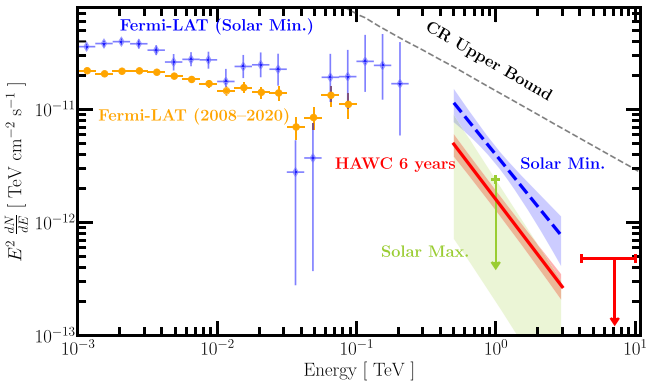

FIG. 3. Spectrum of the solar disk. The 6.1-year spectrum by HAWC is shown by the red solid line. The 90% CL upper limit at 7 TeV is indicated with the red arrow. The spectrum at the solar minimum is indicated by the dashed line. The shaded bands show statistical uncertainties. The solar maximum flux at 1 TeV is shown as the 1σ upper limit. The Fermi-LAT spectra over the full solar cycle [7] (orange) and at the solar minimum [6] (blue) are also shown. The gray dashed line shows the theoretical maximum on the γ-ray spectrum [5].

parameters, we maximize the likelihood in Eq. (2) with respect to A, γ, and r.

We define our test statistic (TS) as

$$\mathrm{TS} = 2[\mathcal{L}(\hat{A}, \hat{\gamma}, \hat{r}) - \mathcal{L}_{\mathrm{Bkg}}], \tag{3}$$

where $\mathcal{L}_{\mathrm{Bkg}}$ is the log-likelihood for the null hypothesis (the background-only scenario) and $\hat{A}$, $\hat{\gamma}$, and $\hat{r}$ are the best-fit values of the model parameters.

Table I shows the results for the full 6.1 years of data, the solar-maximum period, and the solar-minimum period. When restricting to these shorter periods, we fix the disk radius to 0.24°, which is the best-fit value for the full dataset (and close to the true value of 0.26°). A disklike hypothesis shows a slightly higher TS than a simple point source when performing the spectral fit. While the solar minimum flux is higher than that at solar maximum, the spectral slopes are consistent with each other and that for the full dataset. The fitted values of the slope are significantly steeper than that of the cosmic rays. The spectral fits are subject to the systematic errors that result from uncertainties in the modeling of the detector response to air showers. The sources of these uncertainties are discussed in detail in Ref. [23]. In this analysis, they impact the measured flux by ∼15%.

Figure 3 shows the γ-ray spectrum of the Sun obtained with HAWC data. We also show 1–100 GeV Fermi-LAT data over a full solar cycle (August 2008 to February 2020) [7]. Although there is a gap between the energy ranges of Fermi-LAT and HAWC, the comparison of their fluxes, plus the steeper slope for the HAWC data, suggests a break energy at ∼400 GeV, which is another important clue for theoretical modeling.

Conclusions.—Probing the Sun at the highest energies is key to understanding the propagation of cosmic rays in the heliosphere, and in particular to solving the puzzles of the unexpectedly bright GeV γ-ray emission seen by Fermi. Our TeV observations with HAWC show that the Sun continues to be an anomalously bright γ-ray source at very high energies. The observations can be compared to the maximum possible flux assuming all the cosmic rays impinging on the solar surface are reversed and undergo hadronic interactions to produce gamma rays [5]. In fact, the observed flux during solar minimum is ∼20% of the theoretical maximum emission due to cosmic-ray interactions [5], indicating a remarkable efficiency of the underlying mechanism. Moreover, the observed flux is almost 2 orders of magnitude higher than the flux expected from the solar limb alone [10], indicating the important role of magnetic fields in modulating and enhancing the flux.

Our results provide new clues about the emission mechanism. The steeper spectral index than found for Fermi observations indicates a change in the processes, as well as a break energy ∼400 GeV between the two datasets. The measured spectrum of the Sun in HAWC data extends to an estimated maximum energy of 2.6 TeV (see the Supplemental Material [22]). The corresponding cosmic-ray energy of ∼26 TeV sets a new empirical energy scale up to which cosmic rays penetrate the photosphere and produce gamma rays under the influence of magnetic fields.

Models of cosmic ray interactions in the Sun such as Refs. [9,11,12] already underpredict the observed γ-ray flux from the Sun in the GeV range (see however, Ref. [13]). Our observations highlight the need for a revised framework that can explain the anomalous excess of gamma rays from the Sun also in the TeV range.

We thank Jung-Tsung Li for useful comments on the manuscript. We acknowledge the support from the US National Science Foundation (NSF); the US Department of Energy Office of High-Energy Physics; the Laboratory Directed Research and Development (LDRD) program of Los Alamos National Laboratory; Consejo Nacional de Ciencia y Tecnología (CONACyT), México, Grants No. 271051, No. 232656, No. 260378, No. 179588, No. 254964, No. 258865, No. 243290, No. 132197, No. A1-S-46288, No. A1-S-22784, cátedras 873, 1563, 341, 323, Red HAWC, México; DGAPA-UNAM Grants No. IG101320, No. IN111716-3, No. IN111419, No. IA102019, No. IN110621, No. IN110521, No. IN102223; VIEP-BUAP; PIFI 2012, 2013, PROFOCIE 2014, 2015; the University of Wisconsin Alumni Research Foundation; the Institute of Geophysics, Planetary Physics, and Signatures at Los Alamos National Laboratory; Polish Science Centre Grant No. DEC-2017/27/B/ST9/02272; Coordinación de la Investigación Científica de la Universidad Michoacana; Royal Society—Newton Advanced Fellowship 180385; Generalitat Valenciana, Grant No. CIDEGENT/2018/034; The Program Management Unit for Human Resources & Institutional Development, Research and Innovation, NXPO (Grant No. B16F630069); Coordinación General Académica e Innovación (CGAI-UdeG), PRODEP-SEP UDG-CA-499; and the Institute of Cosmic Ray Research (ICRR), University of Tokyo. H. F. acknowledges support by NASA under Award No. 80GSFC21M0002. We also acknowledge the significant contributions over many years of Stefan Westerhoff, Gaurang Yodh, and Arnulfo Zepeda Dominguez, all deceased members of the HAWC collaboration. Thanks to Scott Delay, Luciano Díaz, and Eduardo Murrieta for technical support. The work of J. F. B. was supported by NSF Grant No. PHY-2012955. The work of B. Z. was supported by the Simons Foundation. The work of A. H. G. P., B. Z., K. N., J. F. B., M. N., and T. L. was supported in part by NASA Grant No. 80NSSC20K1354. The work of A. H. G. P. and J. F. B. was additionally supported in part by NASA Grant No. 80NSSC22K0040. The work of T. L. was supported by the ERC under Grant No. 742104, the SNSA under Contract No. 117/19, and VR under Contract No. 2019-05135. The work of K. C. Y. N. is supported by the RGC of HKSAR, Project No. 24302721.

*Corresponding author: nisamehr@msu.edu

[1] National Research Council, *Solar and Space Physics: A Science for a Technological Society* (National Academies Press, New York, 2013).

[2] National Research Council, *Pathways to Discovery in Astronomy and Astrophysics for the 2020s* (National Academies Press, New York, 2021).

[3] A. Abdo *et al.*, Fermi Large Area Telescope observations of two gamma-ray emission components from the quiescent sun, Astrophys. J. **734**, 116 (2011).

[4] Kenny C. Y. Ng, John F. Beacom, Annika H. G. Peter, and Carsten Rott, First observation of time variation in the solar-disk gamma-ray flux with Fermi, Phys. Rev. D **94**, 023004 (2016).

[5] Tim Linden, Bei Zhou, John F. Beacom, Annika H. G. Peter, Kenny C. Y. Ng, and Qing-Wen Tang, Evidence for a New Component of High-Energy Solar Gamma-Ray Production, Phys. Rev. Lett. **121**, 131103 (2018).

[6] Qing-Wen Tang, Kenny C. Y. Ng, Tim Linden, Bei Zhou, John F. Beacom, and Annika H. G. Peter, Unexpected dip in the solar gamma-ray spectrum, Phys. Rev. D **98**, 063019 (2018).

[7] Tim Linden, John F. Beacom, Annika H. G. Peter, Benjamin J. Buckman, Bei Zhou, and Guanying Zhu, First observations of solar disk gamma rays over a full solar cycle, Phys. Rev. D **105**, 063013 (2022).

[8] E. Orlando and A. W. Strong, Gamma-ray emission from the solar halo and disk: A study with EGRET data, Astron. Astrophys. **480**, 847 (2008).

[9] D. Seckel, Todor Stanev, and T. K. Gaisser, Signatures of cosmic-ray interactions on the solar surface, Astrophys. J. **382**, 652 (1991).

[10] Bei Zhou, Kenny C. Y. Ng, John F. Beacom, and Annika H. G. Peter, TeV solar gamma rays from cosmic-ray interactions, Phys. Rev. D **96**, 023015 (2017).

[11] Zhe Li, Kenny C. Y. Ng, Songzhan Chen, Yuncheng Nan, and Huihai He, Simulating gamma-ray production from cosmic rays interacting with the solar atmosphere in the presence of coronal magnetic fields, arXiv:2009.03888.

[12] M. N. Mazziotta, P. De La Torre Luque, L. Di Venere, A. Fassò, A. Ferrari, F. Loparco, P. R. Sala, and D. Serini, Cosmic-ray interactions with the Sun using the FLUKA code, Phys. Rev. D **101**, 083011 (2020).

[13] Miguel Gutiérrez and Manuel Masip, The Sun at TeV energies: Gammas, neutrons, neutrinos and a cosmic ray shadow, Astropart. Phys. **119**, 102440 (2020).

[14] Miguel Gutiérrez, Manuel Masip, and Sergio Muñoz, The solar disk at high energies, Astrophys. J. **941**, 86 (2022).

[15] C. A. Argüelles, G. de Wasseige, A. Fedynitch, and B. J. P. Jones, Solar atmospheric neutrinos and the sensitivity floor for solar dark matter annihilation searches, J. Cosmol. Astropart. Phys. 07 (2017) 024.

[16] Kenny C. Y. Ng, John F. Beacom, Annika H. G. Peter, and Carsten Rott, Solar atmospheric neutrinos: A new neutrino floor for dark matter searches, Phys. Rev. D **96**, 103006 (2017).

[17] Joakim Edsjo, Jessica Elevant, Rikard Enberg, and Carl Niblaeus, Neutrinos from cosmic ray interactions in the Sun, J. Cosmol. Astropart. Phys. 06 (2017) 033.

[18] Rebecca K. Leane, Kenny C. Y. Ng, and John F. Beacom, Powerful solar signatures of long-lived dark mediators, Phys. Rev. D **95**, 123016 (2017).

[19] A. Albert *et al.* (HAWC Collaboration), Constraints on spin-dependent dark matter scattering with long-lived mediators from TeV observations of the Sun with HAWC, Phys. Rev. D **98**, 123012 (2018).

[20] A. Albert *et al.* (HAWC Collaboration), First HAWC observations of the Sun constrain steady TeV gamma-ray emission, Phys. Rev. D **98**, 123011 (2018).

[21] B. Bartoli *et al.* (ARGO-YBJ Collaboration), Search for gamma-ray emission from the Sun during solar minimum with the ARGO-YBJ experiment, Astrophys. J. **872**, 143 (2019).

[22] See Supplemental Material at http://link.aps.org/supplemental/10.1103/PhysRevLett.131.051201 for additional details.

[23] A. U. Abeysekara *et al.* (HAWC Collaboration), Measurement of the Crab Nebula at the highest energies with HAWC, Astrophys. J. **881**, 134 (2019).

[24] K. M. Górski, E. Hivon, A. J. Banday, B. D. Wandelt, F. K. Hansen, M. Reinecke, and M. Bartelman, HEALPix—A framework for high resolution discretization, and fast analysis of data distributed on the sphere, Astrophys. J. **622**, 759 (2005).

[25] Salvatore De Gaetano, Mario Nicola Mazziotta, Francesco Loparco, and Nicola Giglietto (Fermi Large Area Telescope Collaboration), The gamma-ray Moon seen by the Fermi LAT over a full solar cycle, Proc. Sci., ICRC2021 (**2021**) 607.

[26] A. U. Abeysekara *et al.* (The historical and present HAWC Collaboration), The High-Altitude Water Cherenkov (HAWC) observatory in México: The primary detector, Nucl. Instrum. Methods Phys. Res., Sect. A **1052**, 168253 (2023).

[27] A. U. Abeysekara *et al.* (HAWC Collaboration), Observation of the Crab Nebula with the HAWC gamma-ray observatory, Astrophys. J. **843**, 39 (2017).

[28] A. Albert *et al.* (HAWC Collaboration), 3HWC: The third HAWC catalog of very-high-energy gamma-ray sources, Astrophys. J. **905**, 76 (2020).

[29] A. U. Abeysekara *et al.*, Search for very high-energy gamma rays from the northern Fermi bubble region with HAWC, Astrophys. J. **842**, 85 (2017).

[30] A. U. Abeysekara *et al.* (HAWC Collaboration), Multiple Galactic Sources with Emission Above 56 TeV Detected by HAWC, Phys. Rev. Lett. **124**, 021102 (2020).

[31] H. Abdalla *et al.*, TeV emission of galactic plane sources with HAWC and H.E.S.S., Astrophys. J. **917**, 6 (2021).

[32] A. Albert *et al.*, Probing the sea of cosmic rays by measuring gamma-ray emission from passive giant molecular clouds with HAWC, Astrophys. J. **914**, 106 (2021).

[33] A. U. Abeysekara *et al.* (HAWC and IceCube Collaborations), All-sky measurement of the anisotropy of cosmic rays at 10 TeV and mapping of the local interstellar magnetic field, Astrophys. J. **871**, 96 (2019).

[34] R. Alfaro *et al.* (HAWC Collaboration), All-particle cosmic ray energy spectrum measured by the HAWC experiment from 10 to 500 TeV, Phys. Rev. D **96**, 122001 (2017).

[35] A. Albert *et al.* (HAWC Collaboration), A survey of active galaxies at TeV photon energies with the HAWC gamma-ray observatory, Astrophys. J. **907**, 67 (2021).
[36] Igor V. Moskalenko, Troy A. Porter, and Seth W. Digel, Inverse Compton scattering on solar photons, heliospheric modulation, and neutrino astrophysics, Astrophys. J. **652**, L65 (2006).
[37] E. Orlando and A. W. Strong, Gamma rays from halos around stars and the Sun, Astrophys. Space Sci. **309**, 359 (2007).
[38] E. Orlando and A. W. Strong, StellarICS: Inverse compton emission from the quiet Sun and stars from keV to TeV, J. Cosmol. Astropart. Phys. 04 (2021) 004.
[39] R. Atkins *et al.*, Observation of TeV gamma rays from the Crab Nebula with milagro using a new background rejection technique, Astrophys. J. **595**, 803 (2003).
[40] M. Amenomori *et al.* (The Tibet ASγ Collaboration), Evaluation of the Interplanetary Magnetic Field Strength Using the Cosmic-Ray Shadow of the Sun, Phys. Rev. Lett. **120**, 031101 (2018).
[41] M. G. Aartsen *et al.* (IceCube Collaboration), Measurements of the time-dependent cosmic-ray Sun shadow with seven years of IceCube data: Comparison with the Solar cycle and magnetic field models, Phys. Rev. D **103**, 042005 (2021).
[42] T.-P. Li and Y.-Q. Ma, Analysis methods for results in gamma-ray astronomy, Astrophys. J. **272**, 317 (1983).
[43] A. U. Abeysekara *et al.* (HAWC Collaboration), Constraining the p/p ratio in TeV cosmic rays with observations of the Moon shadow by HAWC, Phys. Rev. D **97**, 102005 (2018).
[44] Giacomo Vianello, Robert J. Lauer, Patrick Younk, Luigi Tibaldo, James M. Burgess, Hugo Ayala, Patrick Harding, Michelle Hui, Nicola Omodei, and Hao Zhou, The multi-mission maximum likelihood framework (3 ML), arXiv:1507.08343.
[45] P. W. Younk *et al.*, A high-level analysis framework for HAWC, Proc. Sci., ICRC2015 (**2016**) 948 [arXiv:1508.07479].
[46] Anushka Udara Abeysekara *et al.*, Characterizing gamma-ray sources with HAL (HAWC Accelerated likelihood) and 3 ML, Proc. Sci., ICRC2021 (**2021**) 828.